Characterization of Zn(II)·Deglycobleomycin A_2 and Interaction with $d(CGCTAGCG)_2$: Direct Evidence for Minor Groove Binding of the Bithiazole Moiety

Steven J. Sucheck, Jeffrey F. Ellena, and Sidney M. Hecht*

Contribution from the Departments of Chemistry and Biology, University of Virginia, Charlottesville, Virginia 22901

Received January 16, 1998

Abstract: Deglycobleomycin (dgBLM) binds to and degrades the self-complementary oligonucleotide $d(CGCTAGCG)_2$ in a sequence-selective fashion. To characterize the binding interaction, a 1:1 complex of Zn(II)·dgBLM A_2 with the DNA octanucleotide has been examined using two-dimensional NMR experiments and restrained molecular dynamics calculations. Critical elements of the mode of DNA interaction within two structural domains of Zn(II)·dgBLM A_2 were fundamentally different than those observed previously for Zn(II)·BLM A_2 (Manderville, R. A.; Ellena, J. F.; Hecht, S. M. *J. Am. Chem. Soc*. **1995**, *117*, 7891). A minor groove mode of binding by the bithiazole moiety is supported by the present study. Only slight upfield shifting of the bithiazole (Bit) protons Bit H5 and Bit H5′ is observed, and the sequential intrastrand NOE connectivities are retained upon Zn(II)·dgBLM A_2 binding. The orientation of the drug molecule in the complex is based on the finding of 16 intermolecular Zn(II)·dgBLM A_2−DNA NOEs. The cationic C-substituent of Zn(II)·dgBLM A_2 is positioned in the minor groove of the DNA based on the appearance of 10 NOEs between hydrogens located in the minor groove of DNA and the C-substituent of BLM. Additionally, the results are consistent with the interpretation that the DNA octanucleotide cleavage specificity observed from Fe(II)·dgBLM A_2 and possibly for Fe(II)·BLM A_2 is due in part to recognition of the T_4-A_5 region of the octanucleotide by the bithiazole. Using the NMR-derived NOE distance and dihedral bond angle restraints to guide the molecular dynamics calculations, a binding model for the interaction of Zn(II)·dgBLM A_2 with the octanucleotide has been derived.

The bleomycins (BLMs) are structurally related, glycopeptide-derived antitumor antibiotics originally isolated from a fermentation broth of *Streptomyces verticillus* by Umezawa and coworkers.[1] A mixture of BLMs is used clinically for the treatment of a variety of cancers, notably squamous cell carcinomas, testicular tumors, and non-Hodgkins lymphomas.[2] The therapeutic effect of BLM is believed to result from its ability to mediate DNA[3] and possibly RNA[4] degradation in the presence of a redox-active metal ion cofactor such as Fe[5] or Cu.[6] BLMs (Figure 1) are commonly described by their functional domains. The N-terminus, or metal binding domain, is responsible for metal binding, oxygen binding and activation, and sequence selectivity in DNA binding and cleavage.[7] The disaccharide moiety may also participate in metal ion binding[8] as well as cell surface recognition.[4d] The C-terminus, comprised of the bithiazole (Bit) and the cationic substituent (sulfonium (Sul) in BLM A_2) participates in DNA binding.[9] These two regions are connected by a peptide linker region.

Deglycobleomycin (dgBLM), which lacks the disaccharide moiety (Figure 1), cleaves DNA with a sequence selectivity similar to BLM itself,[10] although with somewhat lesser ef-

(1) (a) Umezawa, H.; Suhara, Y.; Takita, T.; Maeda, K. *J. Antibiot.* **1966**, *19A*, 210. (b) Hecht, S. M. *Acc. Chem. Res*. **1986**, *19*, 383. (c) Stubbe, J.; Kozarich, J. W. *Chem. Rev.* **1987**, *87*, 1107. (d) Natrajan, A.; Hecht, S. M. in *Molecular Aspects of Anticancer Drug−DNA Interactions*; Neidle, S., Waring, M., Eds.; MacMillan: London, 1994; pp 197−242. (e) Kane, S. A.; Hecht, S. M. *Prog. Nucleic Acid Res. Mol. Biol.* **1994**, *49*, 313. (f) Hecht, S. M. in *Cancer Chemotherapeutic Agents*; Foye, W. O., Ed.; American Chemical Society: Washington, 1995; p 369 ff.

(2) *Bleomycin Chemotherapy*; Sikic, B. I., Rozencweig, M., Carter, S. K., Eds.; Academic Press: Orlando, FL, 1985.

(3) (a) D'Andrea, A. D.; Haseltine, W. A. *Proc. Natl. Acad. Sci. U.S.A.* **1978**, *75*, 3608. (b) Takeshita, M.; Grollman, A. P.; Ohtsubo, E.; Ohtsubo, H. *Proc. Natl. Acad. Sci. U.S.A.* **1978**, *75*, 5983. (c) Mirabelli, C. K.; Huang, C.-H.; Crooke, S. T. *Biochemistry* **1983**, *22*, 300.

(4) (a) Carter, B. J.; de Vroom, E.; Long, E. C.; van der Marel, G. A.; van Boom, J. H.; Hecht, S. M. *Proc. Natl. Acad. Sci. U.S.A.* **1990**, *87*, 9373. (b) Holmes, C. E.; Carter, B. J.; Hecht, S. M. *Biochemistry* **1993**, *32*, 4293. (c) Morgan, M. A.; Hecht, S. M. *Biochemistry* **1994**, *33*, 10286. (d) Hecht, S. M. *Bioconjugate Chem.* **1994**, *5*, 513.

(5) (a) Ishida, R.; Takahashi, T. *Biochem. Biophys. Res. Commun*. **1975**, *66*, 1432. (b) Sausville, E. A.; Stein, R. W.; Peisach J.; Horwitz S. B. *Biochemistry* **1978**, *17*, 2740. (c) Sausville, E. A.; Stein, R. W.; Peisach J.; Horwitz S. B. *Biochemistry* **1978**, *17*, 2746.

(6) (a) Ehrenfeld, G. M.; Rodriguez, L. O.; Hecht, S. M.; Chang, C. Basus, V. J.; Oppenheimer, N. J. *Biochemistry* **1985**, *24*, 81. (b) Ehrenfeld, G. M.; Shipley, J. B.; Heimbrook, D. C.; Sugiyama, H.; Long, E. C.; van Boom, J. H.; van der Marel, G. A.; Oppenheimer, N. J.; Hecht, S. M. *Biochemistry* **1987**, *26*, 931.

(7) (a) Sugiyama, H.; Kilkuskie, R. E.; Chang, L.-H.; Ma, L.-T.; Hecht, S. M.; van der Marel, G. A.; van Boom, J. H. *J. Am. Chem. Soc.* **1986**, *108*, 3852. (b) Carter, B. J.; Murty, V. S.; Reddy, K. S.; Wang, S.-N.; Hecht, S. M. *J. Biol. Chem*. **1990**, *265*, 4193. (c) Guajardo, R. J.; Hudson, S. E.; Brown, S. J.; Mascharak, P. K. *J. Am. Chem. Soc*. **1993**, *115*, 7971.

(8) (a) Oppenheimer, N. J.; Rodriguez, L. O.; Hecht, S. M. *Proc. Natl. Acad. Sci. U.S.A.* **1979**, *76*, 5616. (b) Akkerman, M. A. J.; Neijman, E. W. J. F.; Wijmenga, S. S.; Hilbers, C. W.; Bermel, W. *J. Am. Chem. Soc*. **1990**, *112*, 7462.

(9) (a) Chien, M.; Grollman, A. P.; Horwitz, S. B. *Biochemistry* **1977**, *16*, 3641. (b) Povirk, L. F.; Hogan, M.; Dattagupta, N. *Biochemistry* **1979**, *18*, 96. (c) Kross, J.; Henner, W. D.; Haseltine, W. A.; Rodriguez, L.; Levin, M. D.; Hecht, S. M. *Biochemistry*, **1982**, *21*, 3711. (d) Fisher, L. M.; Kuroda, R.; Sakai, T. T. *Biochemistry* **1985**, *24*, 3199.

(10) (a) Sugiyama, H.; Ehrenfeld, G. M.; Shipley, J. B.; Kilkuskie, R. E. Chang, L.-H.; Hecht, S. M. *J. Nat. Prod.* **1985**, *48*, 869. (b) Shipley, J. B.; Hecht, S. M. *Chem. Res. Toxicol.* **1988**, *1*, 25.

S0002-7863(98)00180-2 CCC: $15.00
Published on Web 07/17/1998

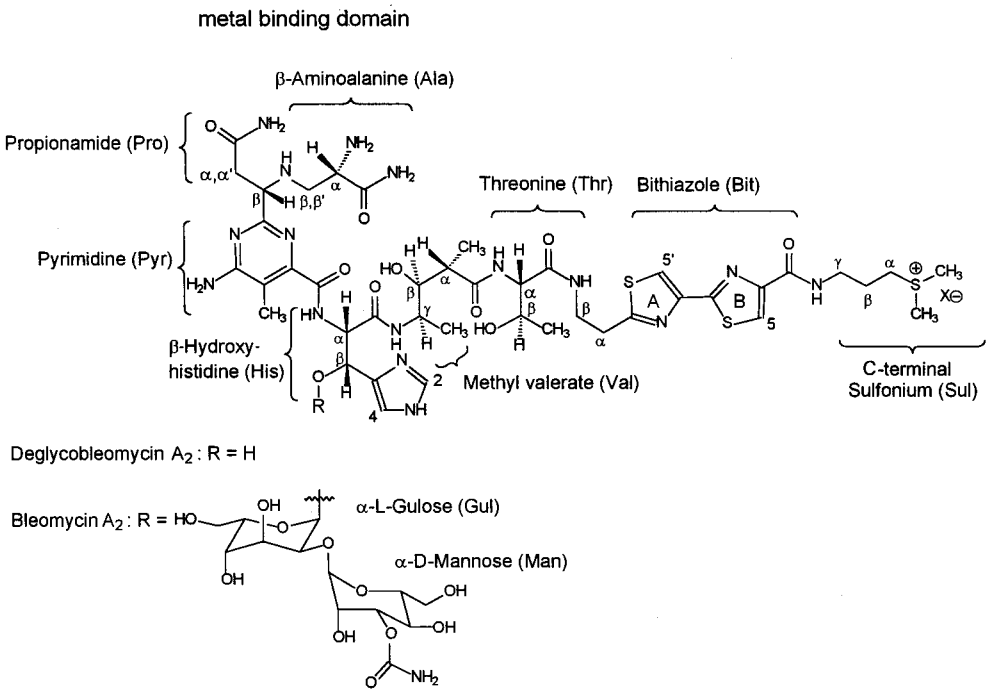

Figure 1. Structures of deglycobleomycin A_2, bleomycin A_2 and designations for individual structural elements.

ficiency and with an altered ratio of single-to-double strand breaks.[11] Deglycobleomycin has also been noted to have altered strand selectivity in the cleavage of a self-complementary oligonucleotide.[7a] DgBLM is an important analogue of BLM because it helps to define the minimum structural elements necessary to perform sequence-selective oxidative DNA degradation.[10,12]

To gain an understanding for the basis of selectivity between dgBLM and BLM, two-dimensional NMR techniques in conjunction with molecular dynamics calculations have been used to study the interaction of Zn(II)·deglycobleomycin A_2 with $d(CGCTAGCG)_2$, which is a particularly good substrate for cleavage by activated metallobleomycins.[7a,13] This system constitutes a reasonable model for the DNA binding of activated metallobleomycins and affords an opportunity to compare the Zn(II)·dgBLM A_2 and Zn(II)·BLM A_2 complexes bound to the same DNA octanucleotide substrate.[14] It also permits interpretation of the NMR data in the context of the available biochemical data for this system.

On the basis of NMR experiments and molecular dynamics calculations, we have developed a model for the binding interaction of Zn(II)·dgBLM A_2 with $d(CGCTAGCG)_2$ that is consistent both with the NMR data and the available biochemical data. The final structure supports a predominantly minor groove binding mode for the bithiazole moiety of Zn(II)·dgBLM A_2 with $d(CGCTAGCG)_2$. The cationic C-substituent also lies exclusively within the minor groove of the DNA substrate.

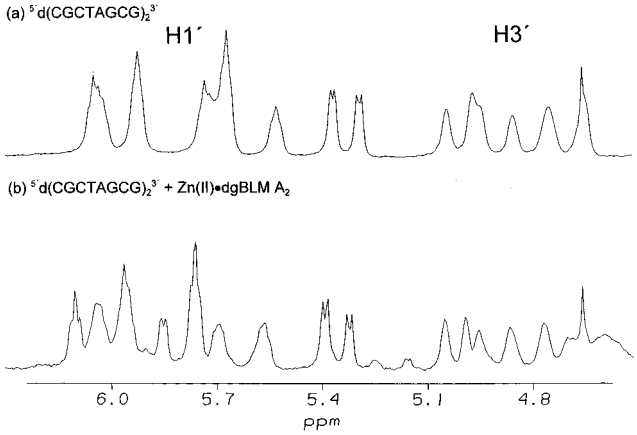

Figure 2. DNA H1′ and H3′ regions (4.5−6.3 ppm) of ^1H NMR spectra of (a) $d(CGCTAGCG)_2$ and (b) the 1:1 complex of Zn(II)·dgBLMA_2−$d(CGCTAGCG)_2$ in D_2O at 35 °C. Samples contained 3.5 mM DNA duplex, pH 6.9, and 20 mM NaCl. Assignments of the DNA deoxyribose H1′ and H3′ regions are indicated in spectrum a.

Results

^1H NMR Assignments. Shown in Figure 2 are the DNA sugar H1′ and H3′ regions of $d(CGCTAGCG)_2$ in D_2O (4.5−6.3 ppm), for both $d(CGCTAGCG)_2$ alone and in the presence of 1 equiv of Zn(II)·dgBLM A_2. The shifting of the resonances upon admixture of Zn(II)·dgBLM A_2 reflects binding of the drug. This is particularly apparent for the H1′ protons of the deoxyribose sugars, which lie in the minor groove of DNA. In contrast, the H3′ protons that lie in the major groove showed very little change upon admixture of Zn(II)·dgBLM A_2. These features are consistent with Zn(II)·dgBLM A_2 binding within the minor groove of the octanucleotide and are analogous to those noted for the previously studied Zn(II)·BLM A_2−$d(CGCTAGCG)_2$ complex. Also evident is the fact that the strands of the self-complementary oligonucleotide remained equivalent, indicating that Zn(II)·dgBLM A_2 is in fast exchange between the symmetry-related binding sites.

(11) Boger, D. L.; Honda, T.; Menezes, R. F.; Colletti, S.-L.; Dang, Q.; Yang, W. *J. Am. Chem. Soc.* **1994**, *116*, 82.

(12) (a) Aoyagi, Y.; Suguna, H.; Murugesan, N.; Ehrenfeld, G. M.; Chang, L.-H.; Ohgi, T.; Shekhani, M. S.; Kirkup, M. P.; Hecht, S. M.; *J. Am. Chem. Soc.* **1982**, *104*, 5237. (b) Sugiura, Y.; Suzuki, T.; Otsuka, M.; Kobayashi, S.; Ohno, M.; Takita, T.; Umezawa, H. *J. Biol. Chem.* **1983**, *258*, 1328. (c) Umezawa, H.; Takita, T.; Sugiura, Y.; Otsuka, M.; Kobayashi, S.; Ohno, M. *Tetrahedron* **1984**, *40*, 501.

(13) (a) Sugiyama, H.; Kilkuskie, R. E.; Hecht, S. M.; van der Marel, G. A.; van Boom, J. H. *J. Am. Chem. Soc.* **1985**, *107*, 7765. (b) Van Atta, R. B.; Long E. C.; Hecht, S. M.; van der Marel, G. A.; van Boom, J. H. *J. Am. Chem. Soc.* **1989**, *111*, 2722.

(14) (a) Manderville, R. A.; Ellena, J. F.; Hecht, S. M. *J. Am. Chem. Soc.* **1994**, *116*, 10851. (b) Manderville, R. A.; Ellena, J. F.; Hecht, S. M. *J. Am. Chem. Soc.* **1995**, *117*, 7891.

Table 1. ^{1}H NMR Chemical Shifts and Coupling Constants of Zn(II)·dgBLM A_2 Complex at 25 °C, pH 6.9 in D_2O

residue	δ (ppm)	J (Hz)	residue	δ (ppm)	J (Hz)
Ala α	3.60	12.8, 2.1	Val αMe	1.13	6.7
Ala β	2.30	12.8, 12.8	Val γMe	1.09	6.4
Ala β'	3.50	12.8, 2.1	Thr α	4.22	4.9
Pro α	2.72	15.1, 8.4	Thr β	4.08	6.0, 6.0
Pro α′	2.82	15.1, 4.3	Thr Me	1.09	6.4
Pro β	4.11	7.0, 4.3	Bit α	3.30	6.1, 6.1
Pyr Me	2.46	s	Bit β	3.63	6.1, 6.1
His α	4.71	6.1	Bit 5	8.20	s
His β	5.17	6.1	Bit 5′	8.09	s
His 2	8.06	s	Sul α	3.39	7.7
His 4	7.34	s	Sul β	2.17	7.6
Val α	2.51	6.9, 6.9	Sul γ	3.57	7.7
Val β	3.63	6.9, 6.1	Sul $(CH_3)_2$	2.92	s
Val γ	3.81	6.4, 6.1			

Table 2. ^{1}H NMR Chemical Shifts (ppm) of Zn(II)·dgBLM A_2, 20 mM NaCl, pH 6.9, in the Absence and Presence of $d(CGCTAGCG)_2$ (+DNA) at 35 °C

residue	Zn(II)·dgBLM A_2	+DNA	$\Delta\delta$
Ala α	3.63	3.66	0.03
Ala β'	3.52	3.52	0.00
Ala β	2.30	2.34	0.04
Pro α	2.71	2.77	0.06
Pro α′	2.80	2.83	0.03
Pro β	4.11	4.12	0.01
Pyr Me	2.47	2.46	−0.01
His α	4.90	4.71	−0.19
His β	5.12	5.17	0.05
His H2	8.09	8.15	0.06
His H4	7.34	7.35	0.01
Val α	2.51	2.51	0.00
Val β	3.66	3.64	−0.02
Val γ	3.81	3.82	0.01
Val αMe	1.12	1.12	0.00
Val γMe	1.08	1.09	0.01
Thr α	4.22	4.22	0.00
Thr β	4.06	4.09	0.03
Thr Me	1.08	1.09	0.01
Bit αH2	3.29	3.20	−0.09
Bit βH2	3.65	3.60	−0.05
Bit 5	8.21	8.06	−0.15
Bit 5′	8.07	7.92	−0.15
Sul αH2	3.37	3.38	0.01
Sul βH2	2.17	2.15	−0.02
Sul γH2	3.59	3.53	−0.06
Sul Me_2^+	2.92	2.93	0.01

Table 1 lists the resonances for Zn(II)·dgBLM A_2 in D_2O at 25 °C; Table 2 lists the resonances at 35 °C for both Zn(II)·dgBLM A_2 alone and in the presence of 1 equiv of $d(CGCTAGCG)_2$. For the free Zn(II)·dgBLM A_2 complex, four resonances corresponding to the bithiazole and β-hydroxyhistidine residues were present. At 35 °C, the β-hydroxyhistidine H2 (His H2) and bithiazole H5 (Bit H5) protons resonated at 8.09 and 8.21 ppm, respectively. Upon addition of the DNA oligonucleotide, the Zn(II)·dgBLM A_2 aromatic resonances broadened, and the bithiazole H5 and H5′ protons shifted upfield from 8.21 and 8.07 ppm to 8.06 and 7.92 ppm, respectively. Compared to the free state, this represents an upfield shift of 0.15 ppm for Bit H5 of the B-ring and 0.15 ppm for Bit H5′ of the A-ring. The absolute magnitudes of chemical shift changes for the bithiazole resonances in Zn(II)·dgBLM A_2 upon admixture of $d(CGCTAGCG)_2$ are significantly less than those observed for either the HOO·Co(III)·BLM A_2−d(CCAGGCCTGG)$_2$[15] or Zn(II)·BLM A_2−$d(CGCTAGCG)_2$[14] complexes as well as the HOO·Co(III)·deglycopepleomycin−CGTACG complex.[16] The HOO·Co(III)·BLM A_2−decanucleotide complex showed upfield shifts for Bit H5 and Bit H5′ resonances of 0.90 and 0.61 ppm, respectively, while the Zn(II)·BLM A_2−octanucleotide Bit H5 and Bit H5′ resonances exhibited upfield shifts of 0.18 and 0.52 ppm, respectively.

Upon cooling the Zn(II)·dgBLM A_2−$d(CGCTAGCG)_2$ complex to 0 °C, the Zn(II)·dgBLM and DNA resonances broaden considerably. However, the Zn(II)·dgBLM A_2 aromatic resonances remain clearly visible (Figure 1, Supporting Information). In contrast, when the temperature was lowered from 35 to 25 °C for Zn(II)·BLM A_2−$d(CGCTAGCG)_2$, the aromatic resonances broadened to the point at which they were no longer visible.[14] These temperature response differences could well reflect the binding of Zn(II)·dgBLM A_2 to the octamer in a single or more limited number of orientations than Zn(II)·BLM A_2. This would also be consistent with the greater selectivity of cleavage observed when using the octanucleotide as substrate for Fe(II)·dgBLM A_2. In any case, the behavior of the Zn(II)·dgBLM A_2−$d(CGCTAGCG)_2$ complex has permitted the acquisition of a 2D NOESY spectrum at 0 °C. Although the complex was still in fast exchange under these conditions, the number and intensity of NOE cross-peaks increased substantially. The additional restraints improved the structure calculation to a degree that was previously unattainable with the Zn(II)·BLM A_2−$d(CGCTAGCG)_2$ complex.[14]

Upon cooling from 35 to 0 °C, the Bit H5 and H5′ protons in the Zn(II)·dgBLM A_2−$d(CGCTAGCG)_2$ complex shifted upfield an additional 0.25 and 0.16 ppm for a total of 0.40 and 0.31 ppm, respectively (Table 1, Supporting Information). The small shifts in the bithiazole ring system are most consistent with an interaction with the DNA involving minor groove binding, which is further stabilized at low temperature. Indeed, netropsin and some of its lexitropsin analogues, which share strong structural similarities with the DNA binding domain of BLM, show upfield chemical shifts of their aromatic hydrogens upon DNA binding of similar magnitude to the shifts observed in these studies.[18]

Also apparent upon admixture of the octamer to Zn(II)·dgBLM A_2 was a downfield shift of His H2 by 0.06 ppm to 8.15 ppm. Shifting of this resonance, as well as other histidine resonances (Table 2), suggests binding to the DNA and further supports earlier evidence that the metal binding domain participates in DNA binding.[7] Assignment of the His H2 and His H4 resonances was achieved from inspection of the DNA titration (Figure 2, Supporting Information) and further verified by the 50-ms TOCSY spectrum of the Zn(II)·dgBLM A_2−$d(CGCTAGCG)_2$ complex (Figure 3, Supporting Information) in which a cross-peak was observed between His H2 and His H4.

Assignments in D_2O and H_2O of the $d(CGCTAGCG)_2$ protons have been made previously by Manderville et al.[14] Proton assignments for Zn(II)·dgBLM A_2 were established by means of DQF−COSY and NOESY experiments carried out in D_2O. Previous chemical shift assignments[19] for all the proton resonances in the Zn(II)·BLM and CO·Fe(II)·dgBLM complexes

(15) Wu, W.; Vanderwall, D. E.; Stubbe, J.; Kozarich, J. W.; Turner, C. J. *J. Am. Chem. Soc.* **1994**, *116*, 10843.

(16) Lui, S. M.; Vanderwall, D. E.; Wu, W.; Tang, X.-J.; Turner, C. J.; Kozarich, J. W.; Stubbe, J. *J. Am. Chem. Soc.* **1997**, *119*, 9603.

(17) In the absence of DNA, only small changes in the chemical shifts of Zn(II)·dgBLM A_2 resonances were noted when the temperature was lowered from 25 °C to 0 °C.

(18) (a) Patel, D. J.; Shapiro, L. *J. Biol. Chem*, **1986**, *261*, 1230. (b) Lee, M.; Krowicki, K.; Hartley, J. A.; Pon, R. T.; Lown, J. W. *J. Am. Chem. Soc.* **1988**, *110*, 3649.

Table 3. ^{1}H NMR Chemical Shifts (ppm) of the DNA Resonances in the Zn(II)·dgBLM A_2−d(CGCTAGCG)$_2$ Complex at 35 °C, pH 6.9, containing 20 mM NaCl[a]

	NH	NH_2	H6/H8	H5/H2	H1′	H2′	H2″	H3′	H4′	H5′, 5″
C1			7.61 (0.09)	5.86 (0.15)	5.77 (0.09)	1.96	2.43 (0.06)	4.70	4.09	3.76
G2	12.87[b] (−0.13)	6.89	7.98		5.96	2.72	2.77	5.00	4.31 (−0.06)	4.13, 4.03
C3		8.19, 6.53 (0.05)	7.61 (0.20)	5.46 (0.09)	5.97 (0.05)	2.06	2.48	4.76	4.07 (−0.19)	4.19
T4	13.65[b] (−0.14)		7.44 (0.07)	1.70	5.57	2.12	2.41	4.88	4.14	4.08
A5			8.22	7.39	6.05	2.76	2.90	5.06	4.41	4.16, 4.05
G6	12.63[b] (−0.11)	6.89	7.69		5.71	2.50	2.60	4.95	4.37	4.21
C7		8.26, 6.41 (0.07), (0.07)	7.27	5.33	5.77	1.85	2.32	4.78	4.08	4.16
G8			7.89 (0.05)		6.11 (0.05)	2.60	2.40	4.67	4.17	4.07

[a] Values in parentheses represent chemical shift changes from free octamer that are ≥ |0.05| ppm. [b] Values obtained at 25 °C.

provided valuable guidance for the assignments made in this study.

Table 2 contains the ^{1}H NMR chemical shifts for Zn(II)·dgBLM A_2 examined at 35 °C in D_2O. The ^{1}H NMR spectrum of Zn(II)·dgBLM A_2 was also assigned when bound to d(CGCTAGCG)$_2$ at 35 °C in a solution containing 20 mM NaCl. The octanucleotide assignments in the presence of Zn(II)·dgBLM A_2 are shown in Table 3. The imino protons of the octanucleotide were assigned in 9:1 H_2O-D_2O in the absence and presence of Zn(II)·dgBLM A_2. Additional assignments of the Zn(II)·dgBLM A_2−d(CGCTAGCG)$_2$ resonances were made at 0 °C (Tables 1 and 2, Supporting Information).

Inspection of Table 2 reveals some general characteristics. Upfield shifts were observed for protons of the bithiazole (Bit) as well as the sulfonium (Sul) substituent (notably Sul γH2, −0.06 ppm) upon DNA binding. This is consistent with a model involving minor groove binding of a cis-oriented bithiazole, with respect to Bit H5 and Bit H5′, and minor groove binding of the cationic C-substituent. Additionally, significant shifting is observed in protons of the β-hydroxyhistidine (His) substituent; these include His αH (−0.19 ppm) and His H2 (0.06 ppm), consistent with the interpretation that the histidine component of the metal binding domain is in close contact with the minor groove of the DNA octanucleotide. Similarly, significant shifting Bit αH2 and Bit βH2 (−0.09 and −0.05 ppm, respectively) resonances are consistent with these moieties interacting with the minor groove of the DNA octanucleotide. The methylvalerate protons show little change in chemical shift, in agreement with models suggesting that this residue is extended away from the helix (vide infra). β-Aminoalanineamide (Ala) and propionamide (Pro) resonances show slight downfield shifting, which may result from their positioning near the minor groove of DNA.

Table 3 shows the ^{1}H chemical shifts of the DNA resonances in the Zn(II)·dgBLM A_2 complex. Compared to the free octanucleotide, only small changes were noted; values in parentheses represent changes of chemical shift for free versus bound octanucleotide that were ≥ |0.05| ppm. Significant downfield shifts were observed for several protons of the base-paired cytidine$_1$ and guanine$_8$ residues, consistent with poor base stacking at the end of the helix. As expected, the most notable shifts involved cytidine$_3$, the major cleavage site for Fe(II)·dgBLM. Downfield shifts were noted at cytidine$_3$ H6 (0.20 ppm), H5 (0.09 ppm), and H1′ (0.05 ppm), consistent with Zn(II)·dgBLM interacting strongly at this base in a minor groove binding mode. Notably, a large upfield shift was observed for cytidine$_3$ H4′ (−0.19 ppm), the hydrogen atom abstracted by Fe(II)·dgBLM at the major site of cleavage; this H is located in the minor groove of DNA. The chemical shifts within cytidine$_3$ provide strong evidence that the metal binding domain of Zn(II)·dgBLM has a bound conformation different from that of Zn(II)·BLM on this octanucleotide substrate since the latter showed pronounced chemical shift changes at cytidine$_7$ H4′. Finally, thymidine$_4$ showed a shift at H6 (0.07 ppm) consistent with the bithiazole interacting with the bases at the T_4-A_5 base step.

DNA Structure. Quantitative and qualitative coupling measurements were obtained from the PE COSY and DQF−COSY experiments carried out on the Zn(II)·dgBLM A_2−DNA complex. From these data, several dihedral angles of the DNA sugars and phosphate backbone could be calculated and used as restraints in the molecular dynamics calculations. The sugar conformations of the oligonucleotide were estimated by the procedure described by Kim et al.[20] and more recently by Schweitzer et al.[21] The procedure relies on an estimation of the deoxyribose coupling constants to apply restraints on the pseudorotation phase angle (P)[22] of the sugar ring for each oligonucleotide. The PE COSY spectrum of the Zn(II)·dgBLM A_2−octanucleotide complex (Figure 4, Supporting Information), was recorded at 35 °C in order to obtain the $J_{H1'-H2'}$ and $J_{H1'-H2''}$ coupling constants. The $J_{H1'-H2'}$ values are larger than the $J_{H1'-H2''}$ values for all sugar residues (Table 3, Supporting Information). This condition restricts the pseudorotation angle to a range of $90° \leq P \leq 198°$.[21] To further restrict the pseudorotation phase angle, the DQF−COSY spectrum of the Zn(II)·dgBLM A_2−d(CGCTAGCG)$_2$ complex was acquired (Figure 5, Supporting Information); $J_{H2'-H3'}$ were less intense than $J_{H1'-H2'}$, reducing the range of the pseudorotation angle to a range of $108° \leq P \leq 198°$. $J_{H3'-H2''}$ and $J_{H3'-H4'}$ cross-peak intensities were practically nonexistent. This condition further restricts the pseudorotational angle to a range of $162° \leq P \leq 198°$.[21] This phase angle range limits the conformations of all the sugars to C2′-*endo* through C3′-*endo* conformations, the

(19) (a) Oppenheimer, N. J.; Rodriguez, L. O.; Hecht, S. M. *Biochemistry* **1979**, *18*, 3439. (b) Oppenheimer, N. J.; Chang, C.; Chang, L.-H.; Ehrenfeld, G.; Rodriguez, L. O.; Hecht, S. M. *J. Biol. Chem.* **1982**, *257*, 1606. (c) Akkerman, M. A. J.; Haasnoot, C. A. G.; Hilbers, C. W. *Eur. J. Biochem.* **1988**, *173*, 211. (d) Calafat, A. M.; Won, H.; Marzilli, L. G. *J. Am. Chem. Soc.* **1997**, *119*, 3656.

(20) Kim, S. G.; Lin, L.-J.; Reid, B. R. *Biochemistry* **1992**, *31*, 3564.

(21) Schweitzer, B. I.; Mikita, T.; Kellogg, G. W.; Gardner, K. H.; Beardsley, G. P. *Biochemistry* **1994**, *33*, 11460.

(22) Altona, C.; Sundaralingam, M. *J. Am. Chem. Soc.* **1972**, *94*, 8205.

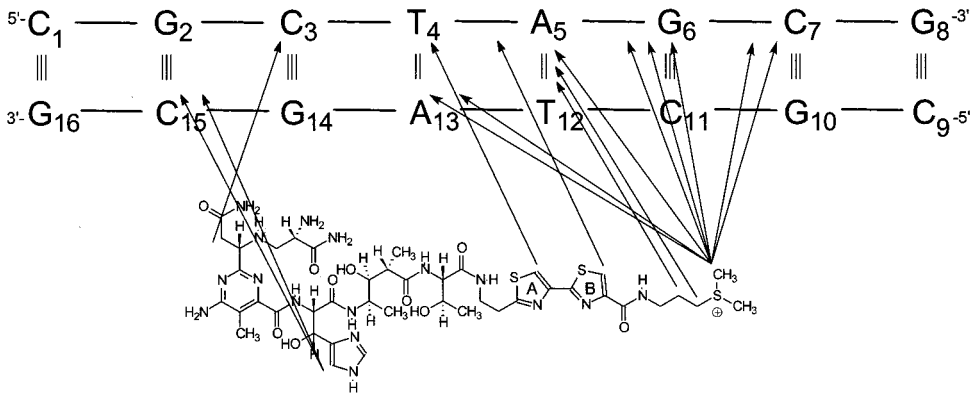

Figure 3. Nucleotide numbering scheme for the Zn(II)·dgBLM A_2−octanucleotide complex and the intermolecular NOEs, represented by arrows, between Zn(II)·dgBLM A_2 and d(CGCTAGCG)$_2$ that were used in the molecular dynamics simulation.

Table 4. Nonvicinal Intermolecular Zn(II)·DgBLM−DNA NOEs and Intramolecular Zn(II)·DgBLM−Zn(II)·DgBLM NOEs in Zn(II)·DgBLM A_2−d(CGCTAGCG)$_2$

intermolecular Zn(II)·dgBLM−DNA NOEs		intramolecular Zn(II)·dgBLM−Zn(II)·dgBLM NOEs		
Sul Me_2^+−A_5 H2	Sul αH2−A_5 H2	Sul Me_2^+−Bit H5	His H2−Ala βH′	His βH−Val γCH_3
Sul Me_2^+−A_{13} H4′	Sul βH2−A_5 H2	Sul Me_2^+−Sul βH2	His H2−Val αH	Pro βH−Ala βH′
Sul Me_2^+−G_6 H4′	Bit H5′−T_4 H2″	Sul Me_2^+−Sul αH2	His H2−Val γCH_3	Pro βH−Ala αH
Sul Me_2^+−C_7 H5′,H5″	Bit H5−A_5 H1′	Sul αH2−Sul γH2	His H2−Val γCH_3	Thr αH−Val αCH_3
Sul Me_2^+−C_7 H4′	Bit H5−G_{14} H1′	Sul βH2−Bit H5	His H4−Val γCH_3	Thr CH_3−Bit H5′
Sul Me_2^+−G_6 H5′,H5″	His H4−C_{15} H2	His H2−Pro αH2	His H4−His βH	
Sul Me_2^+−G_6 H1′	His H4−C_{15} H1′	His H2−Pro βH	His βH−Val αCH_3	
Sul Me_2^+−A_{13} H1′	Pro αH−C_3 H3′	His H2−Ala αH	Thr CH_3−Bit βH2	

typical range for B-form DNA. *P* can be converted into ranges for the individual sugar torsion angles (ν) using the relationship $\nu_j = T_m \cos[P + 144\ (j - 2)]$, where T_m is 35° and *j* is 0−4.[22] These dihedral angles were included in the restrained molecular dynamics calculations.

dgBLM−dgBLM and dgBLM−DNA NOEs. The structure of the free Zn(II)·dgBLM A_2 complex was examined by 2D NMR at 25 °C in D_2O, pH 6.9. The NOESY spectrum (τ_{mix} 300 ms) displayed no notable nonvicinal intramolecular NOEs occurring between the metal binding domain and protons of the linker region. This result suggests that the free Zn(II)·dgBLM A_2 molecule is either extended, highly flexible, or both.

Upon DNA binding, 21 intramolecular Zn(II)·dgBLM−Zn(II)·dgBLM NOEs were assignable at 0 °C (Table 4). Zn(II)·dgBLM A_2−d(CGCTAGCG)$_2$ showed NOEs from the β-hydroxyhistidine (His) H2 and His H4 to the Val γCH_3, suggesting that the methylvalerate moiety is folded in a compact fashion and is in close contact with the metal binding domain. Additional NOEs from the β-hydroxyhistidine were His H2−Val αH and His βH−Val αCH_3. Threonine (Thr) αH also showed an NOE to Val αCH_3. Hydrogen atoms within the metal binding domain exhibited eight intramolecular NOEs. These NOEs define the ligand geometry around the metal center. Again, the majority of key NOEs involved β-hydroxyhistidine. His H2−Ala βH′, His H2−Pro αH2, His H2−Pro βH, and His H2−Ala αH NOEs show that the β-hydroxyhistidine is close to the propionamide and β-aminoalanineamide residues, confirming their proximity to the coordinated Zn(II).

At 0 °C, 16 intermolecular Zn(II)·dgBLM−DNA NOEs were detectable for the Zn(II)·dgBLM A_2−d(CGCTAGCG)$_2$ complex (Table 4). These were used to define the alignment of the drug relative to the helix (Figure 3). Three unambiguous Zn(II)·dgBLM−DNA NOEs involving the C-terminal substituent (Sul Me_2^+, Sul αH2, and Sul βH2) showed contacts to adenosine$_5$ H2 located in the minor groove of DNA; these clearly localize the C-substituent of Zn(II)·dgBLM A_2 in the minor groove of DNA (Figure 3). An additional seven NOEs were observed from the sulfonium substituent to protons located in the minor groove of DNA. NOEs to Sul Me_2^+ were as follows: −A_{13} H1′, −A_{13} H4′, −G_6 H4′, −G_6 H5, −G_6 H1′, −C_7 H5, and −C_7 H4′. No NOE contacts from the C-substituent to the DNA were observed in previous studies of the Zn(II)·BLM A_2−d(CGCTAGCG)$_2$ complex.[14] This is the first direct NOE-derived evidence that the dimethylsulfonium C-substituent can

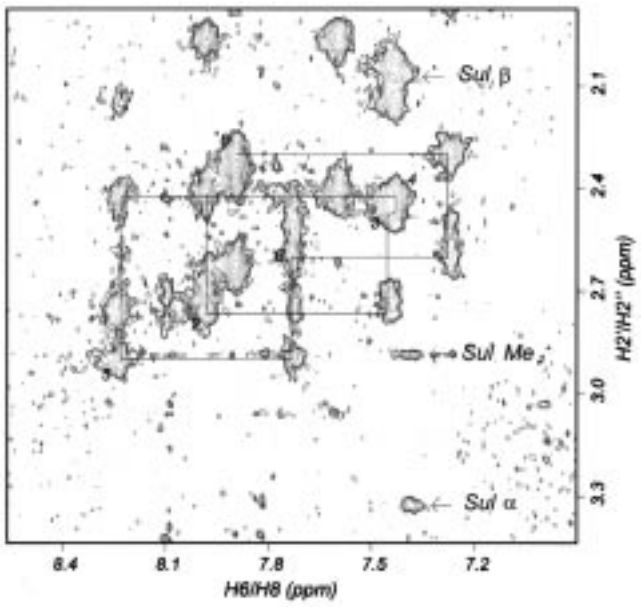

Figure 4. H6/H8−H2′,H2″ region (7.2−8.3 ppm) of the NOESY spectrum of the 1:1 Zn(II)·dgBLM A_2−d(CGCTAGCG)$_2$ complex in D_2O acquired at 0 °C. Key intermolecular Zn(II)·dgBLM A_2−adenosine$_5$ H2 NOEs are indicated. H6/H8−H2′,H2″ NOE connectivies are also indicated: (1) C1 H2″−G_2 H8, (2) G_2 H2″−G_2 H8, (3) C_3 H2″−C_3 H6, (4) T_4 H2″−T_4 H6, (5) A_5 H2″−A_5 H8, (6) G_6 H2″−G_6 H8, (7) C_7 H2″−C_7 H6, (8) C_7H2″−G_8H8.

Table 5. Comparison of Key Coupling Constants for (metallo) DgBLMs

		dgBLM[19b]	Zn(II)·dgBLM	Zn(II)·BLM[19c]	CO·Fe(II)·dgBLM[19b]	CO·Fe(II)·BLM[19b]
propionamide	^2J	−15.3	−15.1	−16.0	−16.3	−16.8
CH−CH_2	^3J	6.0	4.3	6.3	6.0	6.7
	^3J	8.3	8.4	8.4	8.2	7.6
β-aminoalanine	^2J	−13.1	−12.8	−13.1	−13.9	−13.2
CH−CH_2	^3J	5.3	2.1	2.0	3.7	6.8
	^3J	6.5	12.8	3.1	13.0	3.7
β-hydroxyhistidine	^3J	7.6	6.1	2.7	3.4	2.7

assume a minor groove binding mode (see, however, ref 14b for BLM A_5). Careful inspection of the H6/H8 region of the Zn(II)·dgBLM A_2−d(CGCTAGCG)$_2$ complex revealed no NOE contact with bleomycin. Thus, at least for the Zn(II)·dgBLM A_2−d(CGCTAGCG)$_2$ complex, *no* evidence for major groove binding was observed.

Additional evidence for minor groove binding by the bithiazole moiety derives from the sequential DNA NOE connectivities (Figure 4) that are clearly visible. The combination of weak upfield shifting for the bithiazole resonances and the presence of the sequential NOE connectivities at the C_3−T_4 base step is strongly suggestive of minor groove binding. It should be noted that the absence of a H8/H6−H2′,2″ NOE is characteristic of classical intercalation but was not the observation. An NOE cross-peak between Bit H5′ and T_4 H2″ is consistent with binding by the bithiazole in a lexitropsin-like fashion at the thymidine$_4$−adenosine$_5$ base step in the d(CGCTAGCG)$_2$ substrate.[18] A bithiazole fully intercalated at the C_3−T_4 step, which would be predicted by the HOO·Co(III)·BLM A_2 model,[15] would not be expected to show this NOE.

A few NOEs were noted between the metal binding domain and the octanucleotide. Propionamide (Pro) αH shows a weak NOE to cytidine$_3$ H3′. While H3′ is nominally present in the major groove, our modeling showed that this contact was accessible from a minor groove orientation of the propionamide moiety. Therefore, this contact is entirely consistent with the proposed orientation of the metal binding domain in the minor groove. It is the only NOE observed to the base that is cleaved by dgBLM A_2[7a,10a] whereas Zn(II)·BLM A_2 showed three NOEs to the major site of cleavage by BLM A_2 at cytidine$_7$.[7a,10a,13] Histidine H4 shows two NOEs to the DNA octanucleotide at cytidine$_7$ H2′ or H2″ and H1′ in the minor groove of DNA. This is consistent with the downfield shifting observed at His H2. Cytidine$_{15}$ is the major site of cleavage by Fe(II)·BLM A_2 and is ∼12 Å from the Fe(II)·dgBLM A_2-induced cleavage site at cytidine$_3$ on the opposite strand.

The intramolecular Zn(II)·dgBLM−Zn(II)·dgBLM NOEs and intermolecular Zn(II)·dgBLM−DNA NOEs that we have been able to assign for the Zn(II)·dgBLM A_2−d(CGCTAGCG)$_2$ complex are summarized in Table 4. The NOEs were converted into distance ranges and used as restraints to guide the molecular dynamics calculations (Table 4, Supporting Information).

Molecular Modeling. Modeling of the Zn(II)·dgBLM A_2−d(CGCTAGCG)$_2$ complex was carried out using the InsightII/Discover 95 program. To model the dgBLM−metal ion interaction, heme parameters were utilized. The appropriateness of the use of heme parameters to model the dgBLM complex is supported by the fact that dgBLM forms a stable CO·Fe(II)·dgBLM complex that is not unlikely to resemble CO-bound iron porphyrins.[23] Crystallographic studies on five coordinate complexes as well as recent NMR studies on Zn(II)·tallysomycin A[19d] have shown Zn to adopt closely related trigonal bipyramidal and square pyramidal geometries, respectively. Therefore, Zn(II)·bleomycins are expected to be reasonable models for other metallobleomycins that have also been shown to adopt square pyramidal (5-ligand) as well as octahedral (6-ligand) geometries. Furthermore, Coulombic interactions are likely to play a dominant role in the binding energy. This makes the charge of the metal binding domain a more critical factor than its exact structure. The five BLM metal binding ligands that we have identified are regarded as the most likely ligands for both CO·Fe(II)·dgBLM and Zn(II)·dgBLM complexes based on the results of NMR and molecular dynamics studies on the Zn(II)·BLMs and Zn(II)·tallysomycin A[19c,d] as well as HOO·Co(III)·deglycopepleomycin (vide infra) and crystallographic data on Zn(II)[24] and Cu(II)[25] complexes believed to mimic the metal binding domain of dgBLM. Analysis of coupling constants in the metal binding domain (Table 5) argues strongly that the structure of Zn(II)·dgBLM does not vary dramatically from that of CO·Fe(II)·dgBLM.

Using the NOE restraints listed in Table 4 to guide the molecular dynamics calculations, a model for the binding of Zn(II)·dgBLM A_2 to the octanucleotide was determined. Given the small number of the Zn(II)·dgBLM−DNA NOEs in the metal binding region detected for this particular complex, a distance restraint between the metal ion of the Zn(II)·dgBLM A_2 and cytidine$_3$ H4′ was used (between 2 and 6 Å); this seemed reasonable as the metal ion must be within a finite distance of cytidine$_3$ H4′ in order to initiate the observed cleavage via hydrogen atom abstraction. Listings of additional DNA−DNA restraints used in the calculations are provided as Supporting Information (Tables 5 and 6).

Using the molecular modeling procedure described above and in the Experimental Section, 10 structures for the Zn(II)·dgBLM A_2−d(CGCTAGCG)$_2$ complex were generated. The final energies of these complexes fell within a narrow range, and the average pairwise root-mean-square differences (RMSDs) for all atoms of all 10 structures was 0.91 ± 0.37 and 0.79 ± 0.51 Å for backbone atoms. The pairwise RMSDs for all atoms and for backbone atoms are given as Supporting Information (Tables 7 and 8, respectively). A large variation in structure at the metal binding region is a result of the relatively few NOEs observed between the metal binding region and the DNA octanucleotide. This may reflect a large contribution of the DNA binding affinity within the bithiazole + C-substituent; for this complex, the metal binding domain may not be associated as tightly with the DNA as the remainder of the molecule.[9] The minimized average of the 10 structures generated is shown in Figure 5.

Figure 5 shows a minor groove view of the minimized average structure of Zn(II)·dgBLM A_2−d(CGCTAGCG)$_2$ that satisfies all of the NOE restraints. The Zn(II)·deglycobleomycin molecule fits into the minor groove of the DNA with the metal binding region and bithiazole in close contact with the DNA and the methylvalerate γCH3 extended away from the DNA.

(23) Takahashi, S.; Sam, J. W.; Peisach, J.; Rousseau, D. L. *J. Chem. Soc.* **1994**, *116*, 4408.

(24) Kurosaki, H.; Hayashi, K.; Ishikawa, Y.; Goto, M. *Chem. Lett.* **1995**, 691.

(25) Iitaka, Y.; Nakamura, H.; Nakatani, T.; Muraoka, Y.; Fujii, A.; Takita, T.; Umezawa, H. *J. Antibiot.* **1978**, *31*, 1070.

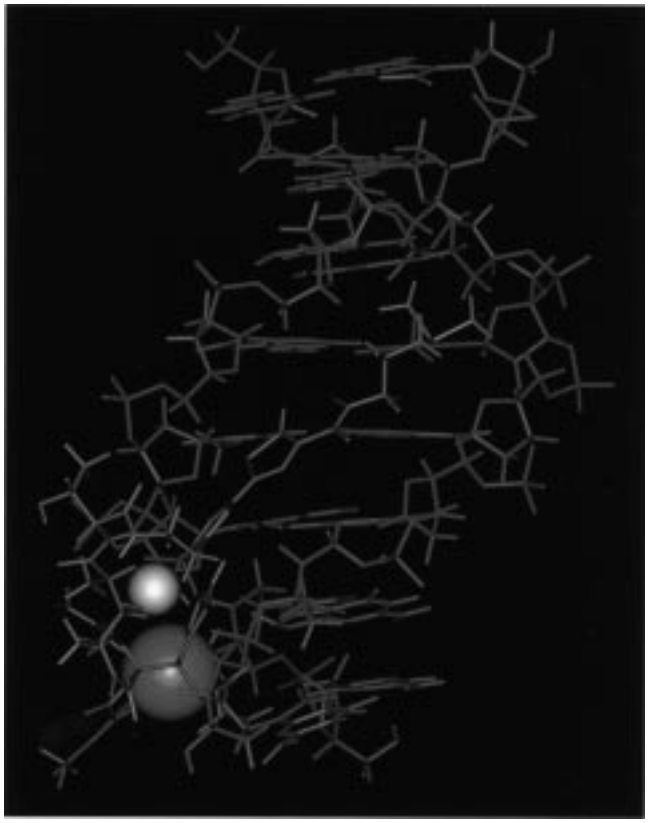

Figure 5. Minor groove view of the model of the Zn(II)·dgBLM A_2 (red)−d(CGCTAGCG)$_2$ (green) complex determined by energy minimization and restrained molecular dynamics calculations. The metal ion of dgBLM (blue sphere) is positioned near the cytidine$_3$ H4′ (yellow sphere).

The bithiazole ring system lies perpendicular to the DNA base pairs. The bithiazole ring system is planar and the cis conformation appears to be preferred. Both trans and cis orientations can be accommodated by a fully minor groove bound orientation of the bithiazole; however, the observed shifts in the bithiazole H5 and H5′ protons cannot easily be accommodated by the trans orientation. The positively charged sulfonium moiety appears to interact with the negatively charged TA tract. The drug molecule contains a bend at the methylvalerate moiety in order to position the metal binding region in the minor groove of the helix.

Figure 6 compares the key interactions between the B-ring thiazole carboxamide and the octanucleotide d(CGCTAGCG)$_2$ and interactions observed for the lexitropsins bound to d(CGCAATTGCG)$_2$. The B-ring thiazolecarboxamide shows bifurcated hydrogen bonding from the Sul NH to A_5 N3 and A_{13} N3 of the octanucleotide. Similar hydrogen bonding patterns are observed from the amide NH of the *N*-methylpyrrolecarboxamide moiety of netropsin, a naturally occurring antibiotic that binds AT-rich DNA sequences, and the closely related lexitropsins.[18,27] In addition, the cationic Sul$(CH_3)_2^+$ of Zn(II)·dgBLM A_2 can participate in an electrostatic interaction with T_{12} O2 of the octamer, analogous to that of netropsin-related compounds bearing a terminal cationic propylguanidinium moiety. NOEs are observed from the methylene hydrogens in the cationic side chain of Zn(II)·dgBLM A_2 to adenosine$_5$ H2 (Figure 4). Similar NOEs are observed in the lexitropsins and netropsin to adenosine H2 protons in the minor groove of DNA (Figure 6). This

(26) Lown, J. W. *Chemtracts*: *Org. Chem.* **1993**, *6*, 205.

(27) Goodsell, D. S.; Kopka, M. L.; Dickerson, R. E. *Biochemistry* **1995**, *34*, 4983 and references therein.

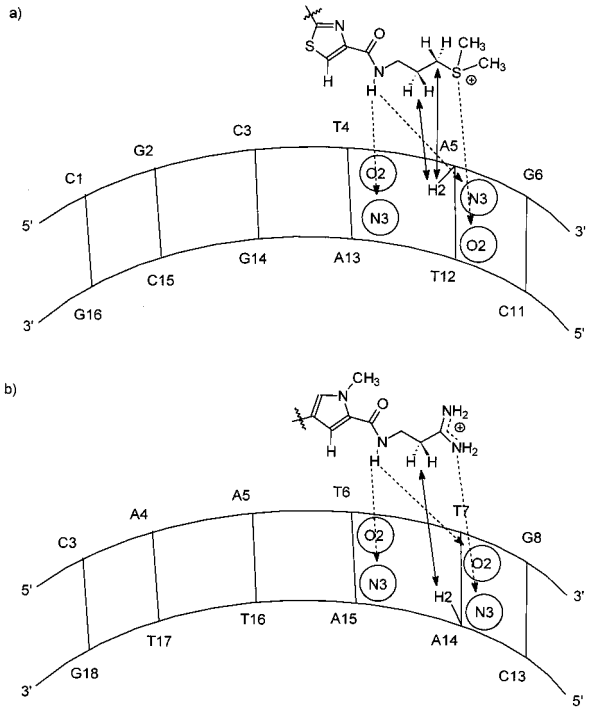

Figure 6. Comparison of (a) the bithiazolecarboxamide of BLMs and (b) *N*-methylpyrrolecarboxamide of lexitropsins.[18] Hydrogen bond and electrostatic interactions (dashed arrows) and NOEs (solid arrows) are indicated.[26]

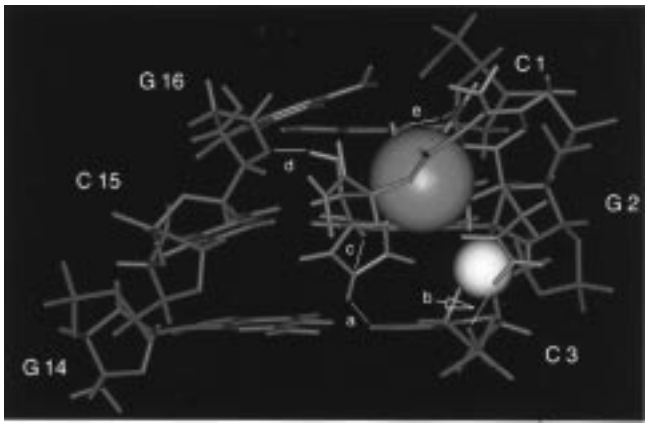

Figure 7. Minor groove view of the d(CGC-)$_2$ region of the Zn(II)·dgBLM A_2−d(CGCTAGCG)$_2$ complex. The metal ion of Zn(II)·dgBLM (blue ball) is positioned near cytidine$_3$ H4′ (yellow ball). Hydrogen bonds (white) are indicated: (a) His N3H−C3 O2, (b) Pro amide NH−T4 PO, (c) His N3−G2 N2H, (d) His OH−G16 O4′, and (e) Ala amide NH to C1 O2.

netropsin-like model for the bithiazole of Zn(II)·dgBLM A_2 is consistent with a cis-oriented bithiazole and the upfield shifting observed for the Bit H5 and Bit H5′ protons.

Despite the small number of NOEs observed from the metal binding domain to the octamer, restrained molecular dynamics calculations produce a metal binding domain that adopts a conformation fully consistent with the biochemical data available on metallobleomycins (Figure 7). Apparent in the figure are several hydrogen bonds between the metal binding domain and the octamer. Hydrogen bonds are observed from (a) His N3H to C_3 O2, (b) Pro NH to T_4 PO, (c) His N3 to G_2 N2H, (d) His OH to G_{16} O4′, and (e) Ala amide NH to C_1 O2. These interactions agree with reports that sequence selectivity originates within the metal binding domain[7] and that guanosine N2

may be an important recognition element for the bleomycins.[28] The metal ion is positioned about 3.8 Å from the cytidine$_3$ H4′ atom whose abstraction initiates DNA degradation.

Discussion

Intercalation,[16,29] partial intercalation,[9b,14,30] and minor groove binding[9d,28,31] have been advanced to describe the nature of the binding of the C-termini of specific metallobleomycins to DNA. In general, unfused aromatic ring systems, linked by bonds with potential torsional freedom, bind to the minor groove of DNA and typically favor AT-rich regions.[32] Although not true in every case, fused aromatic ring systems typically bind to DNA via intercalation and tend to be GC specific.[33] The bithiazole moiety of dgBLM is an unfused aromatic ring system that closely resembles netropsin and related compounds; therefore, it might be expected to bind to DNA by a minor groove binding mechanism. Indeed, our model indicates a potential bifurcated hydrogen bond formed between the amide NH of the sulfonium substituent and adenosine$_5$ N3 and adenosine$_{13}$ N3 of the octamer. This is very similar to the interaction that is in part responsible for the TA tract selectivity of netropsin and related minor groove binding molecules.[18,27,34] From these modeling results combined with chemical footprinting experiments using photoreactive bithiazoles and BLM analogues,[35] it is apparent that TA tracts adjacent to the primary recognition element, 5′-Gpyr3′, are recognized by the tripeptide (threonine−bithiazole−C-substituent) domain of the BLMs.[35] From the model developed for the Zn(II)·dgBLM−d(CGCTAGCG)$_2$ complex (Figure 7), it appears that the metal binding domain recognizes a 5′-Gpyr3′site. When TA tracts are present in proximity to a 5′-Gpyr3′ site, recognition by the metal binding domain and the tripeptide may act synergistically to produce highly specific binding and cleavage. This interpretation is fully consistent with the altered cleavage specificity for BLM caused by admixture of the TA tract binding compound distamycin.[13a,31a]

That the sequence selectivity of DNA degradation noted for dgBLM and BLM need not derive from an intercalative mode of binding is suggested by the phleomycins, a structurally similar group of antitumor antibiotics. These differ from BLMs only in that they contain a thiazolinylthiazole moiety rather than the bithiazole found in the BLMs.[36] The sp^3 carbon in the thiazolinylthiazole moiety necessarily precludes classical intercalation;[9b] the observation that phleomycin and BLM both produce DNA cleavage with essentially identical sequence specificity[37] suggests strongly that intercalation is not an essential feature of the mode of DNA binding and cleavage by bleomycin.

Other lines of evidence suggesting that the interaction of BLM with DNA need not involve full intercalation include the results of Hénichart and co-workers, who demonstrated that the motion of a nitroxide spin-label was disrupted when attached to one ring of the bithiazole but not to the other.[30] These results can be considered as consistent with the preferential shielding of one of the rings of the bithiazole in the Zn(II)·BLM A_2−d(CGCTAGCG)$_2$ model.[14] Further evidence for partial intercalation or minor groove binding derives from a study of helix elongation, which shows that BLM fails to effect viscosity changes in DNA typical of classical intercalation.[9b] In contrast, recent models of HOO·Co·BLM clearly show both thiazoles fully intercalated.[16,29] Our model of preferential minor groove binding based on netropsin-like binding to the minor groove accommodates the results obtained with phleomycin.

Val γCH_3 shows intramolecular NOEs with the β-hydroxyhistidine H2, H4, and βH protons (Table 4), consistent with previous models of BLM A_2,[14,16,29,38d,e,f] which have a bent DNA-bound conformation consisting of a reverse turn at the tripeptide−β-hydroxyhistidine junction with placement of the tripeptide fully bound to DNA from the minor groove side. The observation of several intramolecular NOEs to Val γCH_3 underscores the importance of this structural element of BLM, as previously noted by Umezawa et al.[38] Thus, the methylvalerate substituent appears to facilitate adoption of a productive bound conformation that leads to DNA cleavage. This hypothesis is supported by DNA cleavage studies on several dgBLM A_2 analogues that vary at the methylvalerate substituent.[39] Other recent studies based on 2D NMR spectra of BLM complexed with oligonucleotides also implicate a bent bound conformation.[14,16,29] An interesting feature apparent in the proposed model of Zn(II)·dgBLM A_2 bound to the octanucleotide is that the methylvalerate moiety extends out of the DNA minor groove. This is consistent with data indicating that the tripeptide exhibits the majority of the binding energy observed for BLM itself, with little binding contribution from the methylvalerate or β-hydroxyhistidine moieties in metal free binding studies.[9a] The N-terminal metal chelation domain makes additional stabilizing binding contacts with DNA, as indicated by hydrogen bonds from this domain to the DNA (Figure 7).

Of particular interest are the chemical shifts at the cytidine$_3$ cleavage site upon the addition of Zn·dgBLM A_2. The shift at the cytidine$_3$ H4′ resonance was especially important and indicates the close proximity of the metal binding domain to the major site of cleavage for dgBLM, as opposed to cytidine$_7$

(28) (a) Kuwahara, J.; Sugiura, Y. *Proc. Natl. Acad. Sci. U.S.A.* **1988**, *85*, 2459. (b) Bailly, C.; Waring, M. J. *J. Am. Chem. Soc.* **1995**, *117*, 7311.

(29) (a) Wu, W.; Vanderwall, D. E.; Turner, C. J.; Kozarich, J. W.; Stubbe, J. *J. Am. Chem. Soc.* **1996**, *118*, 1281. (b) Cortes, J. C.; Sugiyama, H.; Ikudome, K.; Saito, I.; Wang, A. H.-J. *Biochemistry* **1997**, *36*, 9995.

(30) Hénichart, J.-P.; Bernier, J.-L.; Helbecque, N.; Houssin, R. *Nucleic Acids Res.* **1985**, *13*, 6703.

(31) (a) Sugiura, Y.; Suzuki, T. *J. Biol. Chem.* **1982**, *257*, 10544. (b) Dickerson, R. E. In *Mechanisms of DNA Damage and Repair: Implications for Carcinogenesis and Risk Assessment in Basic Life Sciences*; Sini, M. G., Grossman, L., Eds.; Plenum Press: New York, 1986; p 245. (c) Hiroaki, H.; Nakayama, T.; Ikehara, M.; Uesugi, S. *Chem. Pharm. Bull.* **1991**, *39*, 2780. (d) Tueting, J. L.; Spence, K. L.; Zimmer, M. *J. Chem. Soc., Dalton Trans.* **1994**, 551.

(32) (a) Dervan, P. B.; *Science* **1986**, *232*, 464. (b) Lown, J. W. *Chemtracts*: *Org. Chem.* **1993**, *6*, 205.

(33) Wilson, W. D.; Li, Y.; Veal, J. M. *Adv. DNA Sequence Specific Agents* **1992**, *1*, 89.

(34) It may be noted that while the essential similarity of the models of DNA interaction by the lexitropsins and bleomycins is suggested strongly by the similarities in chemical shifts noted above, the actual mode of binding of netropsin is also secured by X-ray crystallographic analysis.[27.]

(35) Manderville, R. A.; Zuber, G.; Quada, J. C.; Ellena, J. F.; Hecht, S. M. In preparation.

(36) (a) Takita, T.; Muraoka, Y.; Fujii, A.; Itoh, H.; Maeda, K.; Umezawa, H. *J. Antibiot.* **1972**, *25*, 197. (b) Takita, T.; Muraoka, Y.; Yoshioka, T.; Fujii, A.; Maeda, K.; Umezawa, H. *J. Antibiot.* **1972**, *25*, 755. (c) Takita, T.; Muraoka, Y.; Nakatani, T.; Fujii, A.; Umezawa, Y.; Naganawa, H.; Umezawa, H. *J. Antibiot.* **1978**, *31*, 801. (d) Hamamichi, N.; Hecht, S. M. *J. Am. Chem. Soc.* **1993**, *115*, 12605.

(37) Kross, J.; Henner, W. D.; Hecht, S. M.; Haseltine, W. A. *Biochemistry* **1982**, *21*, 4310.

(38) (a) Otsuka, M.; Kittaka, A.; Ohno, M.; Suzuki, T.; Kuwahara, J.; Sugiura, Y. Umezawa, H.; *Tetrahedron Lett.* **1986**, *27*, 3639. (b) Kittaka, A.; Sugano, Y.; Otsuka, M.; Ohno, M. *Tetrahedron* **1988**, *44*, 2811. (c) Kittaka, A.; Sugano, Y.; Otsuka, M.; Ohno, M. *Tetrahedron* **1988**, *44*, 2821. (d) Ohno, M.; Otsuka, M. In *Recent Progress in the Chemical Synthesis of Antibiotics*; Lukacs, G., Ohno, M., Eds.; Springer-Verlag: New York, 1990; p 387. (e) Otsuka, M.; Masuda, T.; Haupt, A.; Ohno, M.; Shiraki, T.; Sugiura, Y.; Maeda, K. *J. Am. Chem. Soc.* **1990**, *112*, 838. (f) Owa, T.; Haupt, A.; Otsuka, M.; Kobayashi, S.; Tomioka, N.; Itai, A.; Ohno, M.; Shiraki, T.; Uesugi, M.; Sugiura, Y.; Maeda, K. *Tetrahedron* **1992**, *48*, 1193.

(39) Boger, D. L.; Coletti, S. L.; Teramoto, S.; Ramsey, T. M.; Zhou, J. *Bioorg. Med. Chem.* **1995**, *3*, 1281.

H4′ for the Zn(II)·BLM−octamer complex.[14] Thus each of the Zn(II) complexes produced DNA chemical shifts and intermolecular NOEs uniquely involving those DNA nucleotides actually degraded by the respective Fe(II) complexes.[1d,e,7a,13] Other features that emerge from the model include positioning of the bithiazole on the 3′ side of the cleavage site, in agreement with previous literature reports[15,40] and recent modeling studies for HOO·Co(III)·BLM.[16,29] As noted previously, cleavage also occurs to a small extent at cytidine$_7$. The cytidine$_7$ and cytidine$_3$ H4′ atoms are in adjacent positions on opposite sides of the minor groove; however, they are separated by a distance of about 12 Å and are oriented in opposite directions. Cytidine$_7$ cleavage could be accommodated by a single bithiazole binding interaction, which would place the bithiazole 5′ to the cleavage site if one assumes the cationic C-substituent remains bound to the central T_4-A_5 base step, in analogy to what has been proposed for the Zn(II)·BLM−octamer complex.[14] Another possibility would be intercalation of the bithiazole 3′ to the cytidine$_7$ cleavage site between the C_7-G_8 base step. Therefore, the observed change in selectivity could in principle result either from a change in preference for the two binding sites or separate binding modes for the metal binding domain but not the bithiazole. This alternative mode of DNA interaction by the metal binding domain may well be a consequence of a change in the geometry of the metal binding domain. Recently, systematic studies of BLM analogues using optical absorption, circular dichroism, and magnetic circular dichroism have shown that analogues lacking the carbamoyl moiety had altered metal binding domains.[41]

Several proposals for the arrangement of the ligands within the metal binding domain have been presented (**I**−**XI**, Figure 8).[8b,14,19c,d,24,25,42−45] The metal binding domain is believed to consist of a square plane formed by an imidazole nitrogen of β-hydroxyhistidine, the amide of β-hydroxyhistidine, a pyrimidine nitrogen, and the secondary amine of the β-aminoalanine. Two screw senses have been proposed that depend on the face upon which the axial ligand is positioned on the square plane. In Figure 8, the axial ligand is placed on the top of square plane for all structures so that the screw sense can be depicted by arrows that indicate the connectivity of the ligands within the square plane. Crystal structures have been determined for several model compounds designed to mimic the metal binding domain of Co, Zn, and Cu deglycobleomycins, namely for structures **I**,[43] **II**,[24] **III**[25] and **VI**.[44] Interestingly, both screw senses are represented in these crystallographic studies. There is significant confusion regarding the identity of the axial ligand for fully functionalized BLM. It has been proposed that the primary amine of the β-aminoalanineamide moiety, the 3-*O*-carbamoyl group on mannose, or the pyrimidine nitrogen can act as a fifth or sixth axial ligand. Some modeling studies of Zn(II)·BLM[14,19c] and CO·Fe(II)·BLM[8] have used the 3-*O*-carbamoyl group as an axial ligand (models **VIII** and **IX**, respectively). However, a recent NMR derived model using Zn(II)·tallysomycin indicates a preference for the pyrimidine nitrogen as the axial ligand, model **V**.[19d] NMR derived

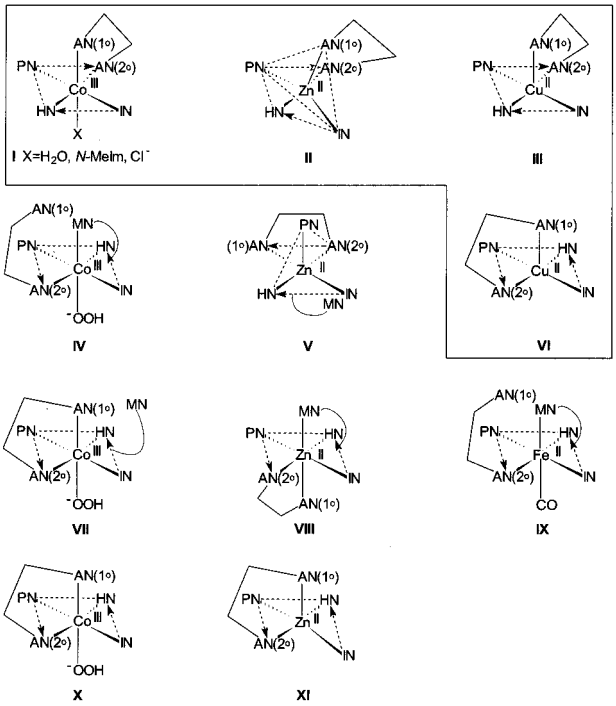

Figure 8. Various metal-binding centers for BLM and dgBLM (see also ref 42). Imidazole nitrogen N1 (IN), the amide of β-hydroxyhistidine (NH), pyrimidine N5 (PN), the secondary amine of β-aminoalanine [AN(2°)], the primary amine of β-aminoalanine [AN(1°)], and the mannose carbamoyl nitrogen (MN) are coordinated to the various metal centers. Crystallographically-derived structures (boxed) for several model compounds designed to mimic the metal binding domain of deglycobleomycins: Co[43] (**I**), *N*-MeIm = *N*-methylimidazole, Zn[24] (**II**), Cu (**III**)[25] and (**VI**).[44] Metal binding domains derived from molecular dynamics calculations: HOO·Co(III)·pepleomycin[42] (**IV**); Zn(II)·tallysomycin[19d] (**V**); HOO·Co(III)·BLM[45] (**VII**); Zn(II)·BLM[14,19c] (**VIII**); CO·Fe(II)·BLM[8b] (**IX**); HOO·Co(III)·deglycopepleomycin[42] (**X**); Zn(II)·dgBLM (**XI**).

molecular dynamics calculations on HOO·Co(III)·BLM[45] indicated that the primary amine was the axial ligand, **VII**. More recently, calculations using HOO·Co(III)·pepleomycin and HOO·Co(III)·deglycopepleomycin indicate that the 3-*O*-carbamoyl group is the axial ligand for HOO·Co(III)·pepleomycin and the primary amine for HOO·Co(III)·deglycopepleomycin, i.e., models **IV** and **X**, respectively.[42]

In the current study, the intramolecular NOEs observed within the metal binding domain in the NOESY spectrum obtained at 0 °C were converted into distance restraints and used in molecular dynamics calculations on Zn(II)·dgBLM in the absence of DNA using the primary amine as the axial ligand. No clear preference for a particular screw sense emerged from these calculations. However, calculations using the full set of intermolecular Zn(II)·dgBLM−DNA and intramolecular Zn(II)·dgBLM−Zn(II)·dgBLM NOE restraints indicated that the screw sense shown in model **XI** is required; this is the same screw sense that has been determined for the other modeling studies (Figure 8).

There are a few possible explanations for the differences between the various BLM models. These include the intrinsic differences between the metal ions in the various metallobleomycins used to model the BLM−DNA interaction, differences between individual BLMs and the dgBLMs, and differences between DNA substrates. Indeed, the possibility that bithiazole−DNA interaction may be sequence dependent is consistent with the results of other similar unfused aromatic systems that are in fast exchange.[18b] For such molecules, it has been

(40) Williams, L. D.; Goldberg, I. H. *Biochemistry* **1988**, *27*, 3004.
(41) Loeb, K. E.; Zaleski, J. E.; Hess, C. D.; Hecht, S. M.; Solomon E. I. *J. Am. Chem. Soc.* **1998**, *120*, 1249.
(42) Cortes, J. C.; Sugiyama, H.; Ikudome, K.; Saito, I.; Wang, A. H.-J. *Eur. J. Biochem.* **1997**, *224*, 818.
(43) Tan, J. D.; Hudson, S. E.; Brown, S. J.; Olmstead, M. M.; Mascharak, P. K. *J. Am. Chem. Soc.* **1992**, *114*, 3841.
(44) Brown, S. J.; Mascharak, P. K. *J. Am. Chem. Soc.* **1988**, *110*, 1996.
(45) (a) Xu, R. X.; Nettesheim, D.; Otvos, J. D.; Petering, D. H. *Biochemistry* **1994**, *33*, 907. (b) Wu, W.; Vanderwall, D. E.; Lui, S. M.; Tang, X.-J.; Turner C. J.; Kozarich J. W.; Stubbe, J. *J. Am. Chem Soc.* **1996**, *118*, 1268.

suggested that drug−DNA complexes exhibiting minor groove binding or intercalation have similar energies.[46] Thus, the T_4−A_5 step provides electrostatics favorable for minor groove binding interactions,[47] while GC-rich sites provide greater opportunity for varying degrees of intercalation. Therefore, we believe the model of DNA binding determined in this study may well reflect the DNA sequence employed.

Experimental Section

The octanucleotide (d(CGCTAGCG)$_2$) was prepared on a DNA synthesizer (Biosearch 8600) using standard phosphoramidite chemistry protocols (15 μmol scale) and purified using preparative silica gel TLC plates (1 mm × 20 cm × 20 cm). The plates were developed using 35:55:10 30% NH_4OH/*i*-PrOH/water. The DNA was eluted from the silica gel with water (15 mL) and isolated. The purification was repeated by preparative silica gel TLC, development with 20:55:25 30% NH_4OH/*i*-PrOH/water. The DNA was desalted on a 5-g Sephadex G-25 column, followed by sodium ion exchange (Dowex 50W ×8 cation-exchange resin). Deglycobleomycin A_2 was prepared from blenoxane by chromatographic fractionation[8a,9a] and deglycosylation[48] as described previously. Deglycobleomycin A_2 was purified by HPLC using a reverse-phase C_{18} column. Elution was effected using a gradient of MeOH in 0.1 M ammonium bicarbonate, pH 7.0.

Sample Preparation. The Zn(II)·dgBLM A_2 complex was prepared by dissolving dgBLM A_2 in 0.5 mL of H_2O (3.5 mM determined spectrophotometrically, ϵ_{292} 14 500 M^{-1} cm^{-1}).[14] To this solution was added 1 equiv of a $ZnSO_4$ solution (144 μL from a 10.8 mM stock solution). The sample was then added to 1 equiv of the octanucleotide (ϵ_{260} 0.812 × 10^5 M^{-1} cm^{-1}). The sample was frozen, lyophilized, and rehydrated in 500 μL of 1:9 D_2O/H_2O containing 20 mM NaCl. For spectra acquired in D_2O, the sample was lyophilized three times from 99.9% D_2O and then redissolved in 100% D_2O.

NMR Experiments. One- and two-dimensional proton NMR experiments were carried out on a General Electric Omega 500 spectrometer operating at 500.13 MHz using external TSP (3-(trimethylsilyl)propionic acid) as reference. In the 2D experiments, the H_2O resonance was suppressed by CW irradiation for 1.5 s, and the sweep width was 5000 Hz. The program Felix (Molecular Simulations Inc., San Diego, CA) running on a Silicon Graphics Crimson Elan workstation was used to process the NMR data. The DQF−COSY spectra[49] contained 256 and 2048 complex points in the t_1 and t_2 dimensions, respectively. Initial processing included apodization in both dimensions with a sine-squared function shifted by 45° and zero filling to 512 points in the t_1 dimension. The PE COSY (E-COSY type) spectra[50] contained 512 and 2048 complex points in t_1 and t_2, respectively, and were acquired with a mixing pulse of 35°. NOESY spectra were obtained at mixing times (τ_{mix}) of 150 and 300 ms. A composite 180° pulse (90_x, 180_y, 90_x) in the middle of the mixing period improved solvent suppression, and 5-ms homospoil pulses were used at the beginning of τ_{mix} and after the composite 180° pulse.[51] The NOESY spectra consisted of 512 and 2048 complex points in the t_2 and t_1 dimensions, respectively; the spectra were apodized with a 3-Hz exponential in t_1 and a 90° shifted sine bell in t_2; t_1 was zero-filled to 1024 points. Homonuclear TOCSY experiments were recorded at 20, 50, and 70 ms.[52]

Analysis of NMR Data. Resonance assignments of Zn(II)·dgBLM A_2 and the octanucleotide d(CGCTAGCG)$_2$ were derived from assessment of the DQF−COSY and NOESY ^{1}H NMR experiments. With the exception of minor variations in the chemical shifts due to temperature and solvent composition, resonance assignments of d(CGCTAGCG)$_2$ were in agreement with those reported previously.[14]

DNA Restraints. In addition to the experimentally derived distance and dihedral restraints obtained from the NMR data, four other types of restraints were used in calculating the structures presented in this study. To preserve the right-handed character of the DNA duplex during the molecular dynamics calculations, the α, β, γ, ϵ, and ζ backbone dihedral angles were restrained to a range covering right-handed B-DNA.[53] To avoid collapse of the major groove during the high-temperature dynamics phase of the simulation, C1 atoms on opposite sides of the major groove were restrained to be greater than 10.87 ± 0.2 Å, and C1 atoms on opposite sides (n +1) of the major groove were restrained to be greater than 13.45 ± 1.0 Å apart during the calculation.[54] Base pairs were kept in Watson−Crick hydrogen-bonded mode by using distance restraints between the bases.[53b] In all, for modeling the Zn(II)·dgBLM A_2−d(CGCTAGCG)$_2$ complex, 15 intermolecular Zn(II)·dgBLM−DNA NOE restraints, 21 intramolecular Zn(II)·dgBLM−Zn(II)·dgBLM NOE restraints, 37 DNA−DNA distance restraints, 152 DNA−DNA dihedral restraints, 328 intramolecular DNA−DNA NOE restraints, 10 Zn(II)·dgBLM and 48 DNA chiral restraints, and a cytidine H4′−metal ion restraint (between 2 and 6 Å) were used. Listings of some of the restraints employed are available in Supporting Information (Tables 4−6). A distance extrapolation method[55] was used to correct for spin diffusion in the DNA−DNA and Zn(II)·dgBLM−Zn(II)·dgBLM distance restraints using the NOE cross-peak volumes from the 150 and 300 ms NOESY spectra. The resulting volumes were converted to distances using the two-spin approximation.[56] The resulting distances were then categorized into small (1−3 Å), medium (2−4 Å), and large (3−5 Å) distance ranges. The Zn(II)·dgBLM−DNA restraints were set to a wide range (1−5 Å) due to the fast exchange nature of the system. Where pseudoatoms were used, an additional 1 Å was added per pseudoatom to account for center-averaging.

Molecular Modeling. Modeling of the interaction of Zn(II)·dgBLM A_2 with the octanucleotide was performed using the Quanta/XPLOR and Insight II/Discover 95 programs and the Biosym CVFF force field. Heme parameters provided with Insight II were used to model the Zn(II)·dgBLM−metal interaction. The five dgBLM ligands identified previously were arranged around the metal center in a square pyramidal arrangement with the primary amine of β-aminoalanine as the axial ligand. The octamer d(CGCTAGCG)$_2$ was constructed in a standard B-form helix using Quanta or Insight II. To provide a starting structure for the Fe(II)·dgBLM−DNA complex, the Fe(II)·dgBLM was docked into the minor groove of the B-form octamer using a standard simulated annealing protocol in Quanta/XPLOR that included Fe(II)·dgBLM−DNA, Fe(II)·dgBLM−Fe(II)·dgBLM, and DNA−DNA distance and dihedral angle restraints. Dynamic distance restraints were used for the Fe(II)·dgBLM−DNA NOEs in order to facilitate the determination of strand assignments. From the resulting structures, the strand assignments were determined.

The simulated annealing protocol was repeated using Insight II/Discover 95. The protocol of restrained dynamics was similar to the one used by Mujeeb et al.[57] and more recently by Schweitzer and co-workers.[21] The atoms of the system were randomized. Then the system was slowly heated to 1000 K. During this high-temperature phase of the simulation, k_{NOE} was slowly increased from 0.5 to 25 kcal mol^{-1} $Å^2$, and the relative weights of all force field terms were reduced to 25%. The system was gradually cooled to 300 K, and the weights of all energy terms were restored to their full values. For the annealing, the dynamics integration step time was 0.5 fs, the cutoff distance for nonbonded interactions was set at 10 Å with a switching distance of 2

(46) (a) Wilson, W. D.; Strekowski, L.; Tanious, F. A.; Watson, R. A.; Mokrosz, J. L.; Strekowska, A.; Webster, G. D.; Neidle, S. *J. Am. Chem. Soc*. **1988**, *110*, 8292. (b) Strekowski, L.; Mokrosz, J. L.; Wilson, W. D.; Mokrosz, M. J.; Strekowski, A. *Biochemistry* **1992**, *31*, 10802.

(47) (a) Zakrzewska, K.; Pullman, B. *Biopolymers* **1986**, *25*, 375. (b) Schmid, N.; Behr, J.-P. *Biochemistry* **1991**, *30*, 4357.

(48) Kenani, A.; Lamblin, G.; Hénichart, J.-P. *Carbohydr. Res*. **1988**, *177*, 81.

(49) Piantini, U.; Sorensen, O. W.; Ernst, R. R. *J. Am. Chem. Soc.* **1982**, *104*, 6800.

(50) Bax, A.; Lerner, L. *J. Magn. Reson.* **1988**, *79*, 429.

(51) Blake, P. R.; Park, J. B.; Bryant, F. O.; Aono, S.; Magnuson, J. K.; Eccleston, E.; Howard, J. B.; Summers, M. F.; Adams, M. W. W. *Biochemistry* **1991**, *30*, 10885.

(52) Bax, A.; Davis, D. G. *J. Magn. Reson*. **1985**, *65*, 355.

(53) (a) Gronenborn, A. M.; Clore, G. M. *Biochemistry* **1989**, *28*, 5978. (b) Baleja, J. D.; Pon, R. T.; Skyes, B. D. *Biochemistry* **1990**, *29*, 4828.

(54) Huang, P.; Eisenberg, M. *Biochemistry* **1992**, *31*, 6518.

(55) Baleja, J. D.; Moult, J.; Skyes, B. D. *J. Magn. Reson.* **1990**, *87*, 375.

(56) Bell, R. A.; Saunders, J. K. *Can. J. Chem.* **1970**, *48*, 1114.

(57) Mujeeb, A.; Kerwin, S. M.; Kenyon, G. L.; James, T. L. *Biochemistry* **1993**, *32*, 13419.

Å, and a distance-dependent dielectric constant of $\epsilon = r_{ij}$ was used. The 10 structures that fit the distance restraints were minimized with several cycles of conjugate gradient minimization. A formal charge of 2+ was assigned to the iron, and primary amines were protonated.

The 10 final structures, all of which satisfied the distance restraints to within 0.3 Å, were derived from these initial structures by energy minimizing with 30 000 cycles of conjugate gradient minimization to a final root-mean-square derivative of <0.001 kcal mol^{-1} Å^{-2}. The effect of solvent was approximated by a distance dependent dielectric constant $\epsilon = 4r_{ij}$ and by reducing the net charge on the phosphate group to -0.32e.[58] These 10 structures were averaged, and the resulting structure was minimized with 30 000 cycles of conjugate gradient minimization to a final root-mean-square derivative of <0.001 kcal mol^{-1} Å^{-2}.

(58) Tidor, B.; Irikura, K. K.; Brooks, B. R.; Karplus, M. *J. Biomol. Struct. Dyn.* **1983**, *1*, 231.

Acknowledgment. This study was supported by Research Grant CA53913 from National Cancer Institute.

Supporting Information Available: ^{1}H NMR, TOCSY, and COSY spectra and chemical shifts, coupling constants, bond distances, and bond angles (17 pages, print/PDF). See any current masthead page for ordering information and Web access instructions.

JA9801801